ARCHIVES OF TRANSPORT *ISSN (print):* *0866-9546*
Volume 41, Issue 1, 2017 ***e-ISSN (online):*** *2300-8830*
DOI: *10.5604/01.3001.0009.7386*

MECHANICAL ANALYSIS AND RESEARCH OF THE CONVEYOR BELT OF PLANE TURNING BELT CONVEYOR BASED ON DISCRETE ELEMENT METHOD

De-yong Li[1], Shuang Wang[2], Kun Hu[3]

[1,2] Anhui University of Science and Technology, Anhui Mine Electromechanical Equipment Cooperative Innovation Center, Huainan China

[3] The Chinese University of Hong Kong, Department of Mechanical and Automation Engineering, Hong Kong

[1]e-mail: ldyziyou@126.com

Abstract: *In view of the size and the change of the load force of the conveyor belt at the turning point of the plane turning belt conveyor, the influencing factors of the stress of the conveyor belt at the turning point of the plane turning belt conveyor under full load condition are analyzed. A three dimensional model of the turning point of the plane turning belt conveyor is established. Combined with previous research experience, the formula for calculating the load is put forward. Based on discrete element method, multiple sets of internal curve elevation angle and the belt speed are used for dynamic simulation analysis. The results showed that the middle of conveyor belt is the most stressed, the lateral force second, the force of the inner conveyor belt is the least. Outside force increases with the increase of speed; there is no change in the middle band; the inner band force decreases with the increase of the velocity. Outside force decreases with the decrease of the inclination angle. With the change of the inclination angle, the force is basically unchanged. With the decreasing of the inclination angle, the force increases gradually. By optimizing the design parameters of the plane turning belt conveyor, the force of belt is reduced, and the service life of belt is improved.*

Key words: *plane turning belt conveyor, conveyor belt force, Discrete Element Method, optimization design.*

1. Introduction

Belt conveyor generally use straight line layout, however, there are some occasions due to the external factors such as terrain constraints, the belt conveyor cannot be used for linear transportation (Rocha et al., 2012) Therefore, the curve conveyor belt conveyor emerges (Pang & Lodewijks, 2007). The curve layout of the existing belt conveyor generally adopts series connection, forced to change direction and natural change direction, which means to change the natural setting conveyor roller group forward, elevation curve and other measures to make the realization of nature oriented conveyor, in place of a plurality of overlapping conveyor transfer modes. This can not only reduce the overlap of belt conveyor, reduce the investment of the driving device, but also reduce dust pollution (Wang, Yang & Song, 2014; Tao, 2013). The analysis of the force of the conveyor belt in the turning section is directly related to the normal operation of the belt conveyor, therefore, the stress analysis of the conveyor belt in the plane turn has attracted the attention of many researchers both at home and abroad. German scholar Holger Lieberwirth (1994) analyze the stress of the adhesive tape and the material in the horizontal turning section has only considered the slot angle and the elevation angle, and has not considered the influence of the rake angle of the roller. Austria scholars Grimmerk and Kessler (1992) carried out the design and calculation of the possible two kinds of limit position, analyzed the large plane turning belt conveyor by dynamic design method, which can improve the design level, avoid the design defects of the traditional design method and the occurrence of the accident. In recent years, Domestic scholars have carried out some researches on the plane turning belt conveyor. Professor Sun Ke-wen (1991) analyzed two dimensional stresses of the conveyor belt and the material in the horizontal turning section, and derived the belt tension and turning radius in the horizontal curve section. Professor Song (Song, 1996; Song et al., 2005; Wang & Song, 2005) analyzed the dynamic characteristics of the large belt conveyor starting from the plane turning and compared with the linear transportation belt conveyor, which obtained the

influence of the turning conveyor on the belt conveyor. Piao Xiang-lan et al., (2007) researched the tape and the material in the horizontal curve section of the stress, although considered the roller forward influence on the force, its mechanical model is not general. At present, the study of the dynamics of the plane turning belt conveyor is still relatively few.

2. Mechanical model of plane turning conveyor belt

2.1. General assumption

Under the actual conditions, the turning point of the belt conveyor adopts the three roll form of the bearing segment groove type roller group. There are two kinds of running state of groove type bearing support roller group, which is load operation and no-load operation. The difference between the load and no-load operation is that the load operation of the material needs to be part of the force calculation by gravity. Therefore, the three section roller type roller group is selected as the research object.

2.2. Force calculation of conveyor belt in plane turning

The necessary condition for the plane turning of the belt conveyor is the force balance at the turning point. Set F_T as the conveyor belt centripetal force of plane turning belt conveyor in one roller spacing, N; R as the radius of curvature at the corner of the plane, m; l_0 as the distance between the support roller group at the turn of the plane, m; v as the belt speed of belt conveyor, m/s.

$$F_T = \frac{mv^2}{R} \tag{1}$$

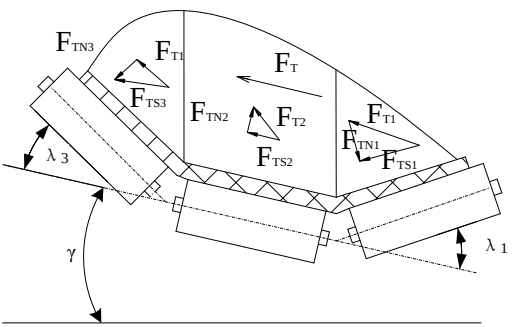

Fig.1. Schematic diagram of material centering force

The analysis (Liu, 2013) indicates that the F_T parallel the supporting roller group surface elevation, and divided the force into the following three components according to the conveyor belt in each roller width, then

$$\begin{cases} F_{T1} = \dfrac{l_{B1}}{B} \cdot F_T = \dfrac{l_{B1}}{B} \cdot \dfrac{mv^2}{R} \\ F_{T2} = \dfrac{l_{B2}}{B} \cdot F_T = \dfrac{l_{B2}}{B} \cdot \dfrac{mv^2}{R} \\ F_{T3} = \dfrac{l_{B3}}{B} \cdot F_T = \dfrac{l_{B3}}{B} \cdot \dfrac{mv^2}{R} \end{cases} \tag{2}$$

The force along roller axial which let the conveyor belt shift to the inside as following:

$$\begin{cases} F_{TS1} = \dfrac{l_{B1}}{B} \cdot F_T = \dfrac{l_{B1}}{B} \cdot \dfrac{mv^2}{R} \cdot \cos(\lambda_1 + \gamma) \\ F_{TS2} = \dfrac{l_{B2}}{B} \cdot F_T = \dfrac{l_{B2}}{B} \cdot \dfrac{mv^2}{R} \cdot \cos\gamma \\ F_{TS3} = \dfrac{l_{B3}}{B} \cdot F_T = \dfrac{l_{B3}}{B} \cdot \dfrac{mv^2}{R} \cdot \cos(\lambda_3 - \gamma) \end{cases} \tag{3}$$

F_T along the normal force of roller which make conveyor belt have a positive pressure on the roller and increase the roller friction. The component force is helpful for conveyor belt turn. Take all the forces as

$$\begin{cases} F_{TN1} = \dfrac{l_{B1}}{B} \cdot F_T = \dfrac{l_{B1}}{B} \cdot \dfrac{mv^2}{R} \cdot \sin(\lambda_1 + \gamma) \\ F_{TN2} = \dfrac{l_{B2}}{B} \cdot F_T = \dfrac{l_{B2}}{B} \cdot \dfrac{mv^2}{R} \cdot \sin\gamma \\ F_{TN3} = \dfrac{l_{B3}}{B} \cdot F_T = \dfrac{l_{B3}}{B} \cdot \dfrac{mv^2}{R} \cdot \sin(\lambda_3 - \gamma) \end{cases} \tag{4}$$

In the formula, B is the width of conveyor belt, m; l_{b1} is the width of conveyor belt on the inner roller, m; l_{b2} is the width of the conveyor belt on the middle roller, m; l_{b3} is the width of the conveyor belt on the outer roller, m; λ_1 is roller group for groove angle, º; λ_2 is the outer roller group groove angle, º; γ is internal curve elevation angle, that is, the theory of slope angle,º.

2.3. Force calculation of material in plane turning

Because of the characteristics of the bulk material, it is decided that the conveyor belt is loose and has certain fluidity. Material is different from the conveying belt at the time of operation and material on conveyor belt in addition to the gravity. And the friction force between the conveyor belt and material. So the analysis of the structure of the plane turn needs to be separated from the conveyor belt and the material.

When the material is turning along with the conveyor belt, due to the relative motion the horizontal relative position of the material and the conveyor belt has been changed. And because the material is continuous, the cross-sectional area of the material is constant, and the cross section of the material is still the same. And the curve radius of the arc, the maximum height of the material and the width of the material are all the same.

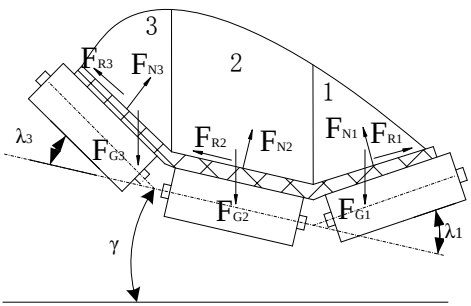

Fig. 2. Schematic diagram of the gravity and friction force of the material and the conveyor belt

When running the material on the groove type supporting roller group, the cross section of the material is approximated as a combination of a trapezoidal cross section and a section of the chord. The roller is divided into three parts, and its bearing capacity is shown in Figure 2.

Set F_{GB1}、F_{GB2} and F_{GB3} in turn for the 3 regions of the conveyor belt gravity, set F_{GG1}、F_{GG2} and F_{GG3} are 3 regions for the gravity of the material, set F_{G1}、F_{G2} and F_{G3} in turn for the total gravity of 3 regions.

$$\begin{cases} F_{G1} = F_{GB1} + F_{GG1} \\ F_{G2} = F_{GB2} + F_{GG2} \\ F_{G3} = F_{GB3} + F_{GG3} \end{cases} \quad (5)$$

According to the literature (Song, Xu & Wang, 2014) available, the conveyor belt gravity calculation is as follows:

$$\begin{cases} F_{GB1} = q_B g l_0 \dfrac{l_{B1}}{B} \\ F_{GB2} = q_B g l_0 \dfrac{l_{B2}}{B} \\ F_{GB3} = q_B g l_0 \dfrac{l_{B3}}{B} \end{cases} \quad (6)$$

The type (6) according to the axial and radial roller conveyor belt is decomposed along the gravity roller axial force as follows:

$$\begin{cases} F_{GBS1} = q_B g l_0 \dfrac{l_{B1}}{B} \sin(\lambda_1 + \gamma) \\ F_{GBS2} = q_B g l_0 \dfrac{l_{B2}}{B} \sin\gamma \\ F_{GBS3} = q_B g l_0 \dfrac{l_{B3}}{B} \sin(\lambda_3 - \gamma) \end{cases} \quad (7)$$

Similarly, the conveyor belt along the gravity roller radial component as follows:

$$\begin{cases} F_{GBN1} = q_B g l_0 \dfrac{l_{B1}}{B} \cos(\lambda_1 + \gamma) \\ F_{GBN2} = q_B g l_0 \dfrac{l_{B2}}{B} \cos\gamma \\ F_{GBN3} = q_B g l_0 \dfrac{l_{B3}}{B} \cos(\lambda_3 - \gamma) \end{cases} \quad (8)$$

In the formula, l_{B1}, l_{B2} and l_{B3} are the contact width of the 3 rollers and conveyor belt respectively, m.

The vertical component of the material gravity effect on the three rollers was measured by the (Piao, 2010) in the literature. The section material is divided into three parts, which are corresponding to the three rollers. Measure the weight of the material on each roller: $k_1 q_G g l_0$, $k_2 q_G g l_0$, $k_3 q_G g l_0$, thereinto, $k_1 + k_2 + k_3 = 1$.

The gravity of the material is decomposed into two forces along the radial and axial direction of the roller, then the calculation formula for the axial component of roller.

$$\begin{cases} F_{GGS1} = k_1 q_G g l_0 \sin(\lambda_1 + \gamma) \\ F_{GGS2} = k_2 q_G g l_0 \sin\gamma \\ F_{GGS3} = k_3 q_G g l_0 \sin(\lambda_3 - \gamma) \end{cases} \quad (9)$$

Similarly, the calculation formula for the radial force of roller as follow,

$$\begin{cases} F_{GGN1} = k_1 q_G g l_0 \cos(\lambda_1 + \gamma) \\ F_{GGN2} = k_2 q_G g l_0 \cos\gamma \\ F_{GGN3} = k_3 q_G g l_0 \cos(\lambda_3 - \gamma) \end{cases} \quad (10)$$

Set F_{N1}、F_{N2} and F_{N3} are in turns as the force of three rollers acting on the belt, then

$$\begin{aligned} F_{N1} &= F_{TN1} + F_{GBN1} + F_{GGN1} = \\ &= \frac{l_{B1}}{B}\frac{mv^2}{R}\sin(\lambda_1 + \gamma) + q_B g a_0 \frac{l_{B1}}{B}\cos(\lambda_1 + \gamma) + \\ &+ k_1 q_G g l_0 \cos(\lambda_1 + \gamma) \end{aligned} \quad (11)$$

$$\begin{aligned} F_{N2} &= F_{TN2} + F_{GBN2} + F_{GGN2} = \\ &= \frac{l_{B2}}{B}\frac{mv^2}{R}\sin(\lambda_1 + \gamma) + q_B g l_0 \frac{l_{B2}}{B}\cos\gamma + \\ &+ k_2 q_G g l_0 \cos\gamma \end{aligned} \quad (12)$$

$$\begin{aligned} F_{N3} &= F_{TN3} + F_{GBN3} + F_{GGN3} = \\ &= \frac{l_{B3}}{B}\frac{mv^2}{R}\sin(\lambda_1 + \gamma) + q_B g l_0 \frac{l_{B2}}{B}\cos\gamma + \\ &+ k_3 q_G g l_0 \cos(\lambda_3 - \gamma) \end{aligned} \quad (13)$$

Set F_{R1}、F_{R2} and F_{R3} as the three roller friction effect on the conveyor belt, μ as the coefficient of friction, then

$$F_{R1} = \mu \cdot F_{N1} = \mu\left[\begin{aligned} &\frac{l_{B1}}{B}\frac{mv^2}{R}\sin(\lambda_1 + \gamma) + q_B g a_0 \frac{l_{B1}}{B}\cos(\lambda_1 + \gamma) + \\ &+ k_1 q_G g l_0 \cos(\lambda_1 + \gamma) \end{aligned}\right] \quad (14)$$

$$F_{R2} = \mu \cdot F_{N2} = \mu\left[\begin{aligned} &\frac{l_{B2}}{B}\frac{mv^2}{R}\sin(\lambda_1 + \gamma) + q_B g l_0 \frac{l_{B2}}{B}\cos\gamma + \\ &+ k_2 q_G g l_0 \cos\gamma \end{aligned}\right] \quad (15)$$

$$F_{R3} = \mu \cdot F_{N3} = \mu\left[\begin{aligned} &\frac{l_{B3}}{B}\frac{mv^2}{R}\sin(\lambda_1 + \gamma) + q_B g l_0 \frac{l_{B3}}{B}\cos\gamma + \\ &+ k_3 q_G g l_0 \cos(\lambda_3 - \gamma) \end{aligned}\right] \quad (16)$$

2.4. Analysis

From formula (11) ~ (16),

①When the belt conveyor in the plane turn, the conveyor belt is supported by the support force (F_{N1}、F_{N2} and F_{N3}) and friction (F_{R1}、F_{R2} and F_{R3}) of the roller group, that is, the total force of the conveyor belt is the vector of the support force and the friction force.

② The total force of the conveyor belt is nonlinear with the speed of the belt, which increases with the increase of the v, and the increment gradually increased. The total force of the conveyor belt is also nonlinear relation with the elevation angle of the inner curve γ, which decreases with the increase of the γ, and the reduction is a trend of fluctuations.

3. EDEM modeling

3.1. Plane turning belt conveyor model

By making use of Solidworks, the author establishes a 3D model of the conveyor belt in transportation, maps the complete machine model in the modern discrete element model software EDEM (Kruggel-Eden et al., 2007), as shown in Fig. 3. Belt conveyor turning length is approximately 5.3m, the bandwidth is 0.8m, the average transport inclination is 0.74 degrees, the spacing of the roller group is 0.6m, the belt speed is 1m/s, the horizontal turning radius is 2.1m, the elevation angle of the internal curve is 5 degrees.

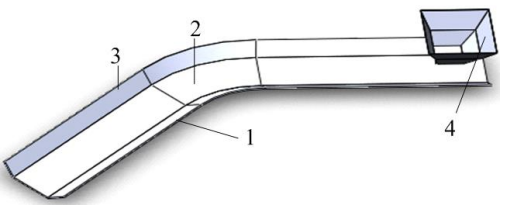

Fig. 3. Three-dimensional model (1.Lateral conveyor belt 2. Middle conveyor belt; 3.Inside conveyor belt)

3.2. Establishment of contact model

In order to accurately describe the contact and crash process between coal material and conveyor belt, as

well as those between coal material and coal material, the granular distinct element method generally adopted the elastic-damping-frictional contact mechanical model, as shown in Fig. 4.

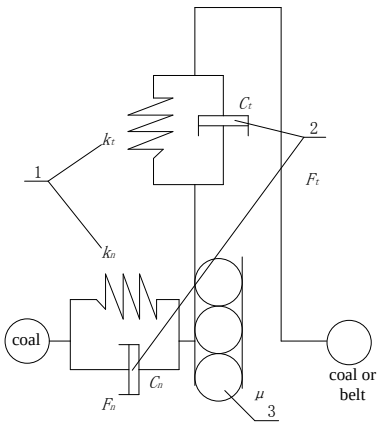

Fig. 4. Contact mechanics model
(F_n is normal force ; F_t is tangential force ; k_n is the normal stiffness ; k_t is shear stiffness ; C_n is the normal damping coefficient ; C_t is the shear damping coefficient ; μ is friction coefficient ;
1. Coal rigidity (spring) ; 2. Damper ; 3. Scraper)

4. Simulation Analysis

4.1. Simulation parameter settings

The uneven granularity of raw coal and mixed gangue after mining makes the separation more difficult. For this reason, lumps of raw coal and mixed gangue should undergo primary breakup before being transported by belt conveyor. In general terms, a jaw breaker can reduce the lump coal to the size ranging from 18mm to 48mm (Li, Du & Xu, 2011), so the size of the simulated coal material is 40mm. Conveyor belt model using Moving-Plane model in order to simulate linear motion of the conveyor belt. The recovery coefficient of each material is set to: between coal and coal is 0.5, between coal and belt is 0.45; the static friction coefficient of each material is set to: between coal and coal is 0.6, between coal and belt is 0.5; the coefficient of rolling friction of each material is set to: between coal and coal is 0.05, between coal and belt is 0.05; The basic material flow parameters: the production rate of the particle factory is 1050 particles/s, simulation time is 10s.

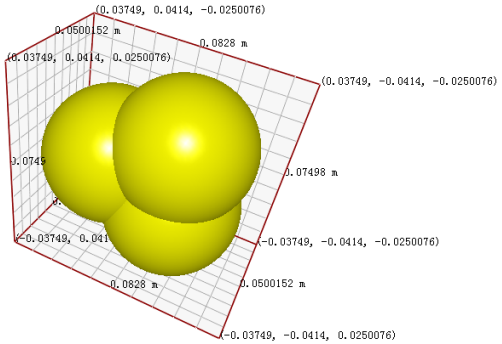

Fig. 5. Coal filling effect diagram

Table. 1. The material mechanical properties

Material	Poisson's ratio	Shear modulus /MPa	Density/(kg/m^3)
coal-coal	0.5	0.6	0.05
coal-belt （ruby）	0.45	0.5	0.05

4.2. Discrete element simulation

EDEM software will automatically calculate the Rayleigh time step, the $0.1T_R$ is chosen as the time step (Živaljić Nikolić & Smoljanović, 2014). Figure 6 is the plane turning belt conveyor transport simulation process, and the real-time quantity in the belt can be displayed during simulation. The measuring area is divided into three parts, and lateral pressure of inside belt, middle belt and outside belt is measured accordingly.

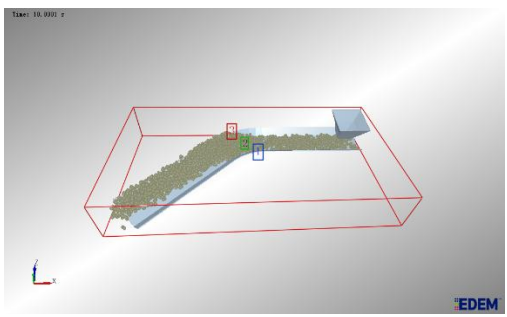

Fig. 6. Simulation process
(1. Measurement area of the inner conveyor belt; 2. Measurement area of the middle conveyor belt; 3. Measurement area of the outside conveyor belt)

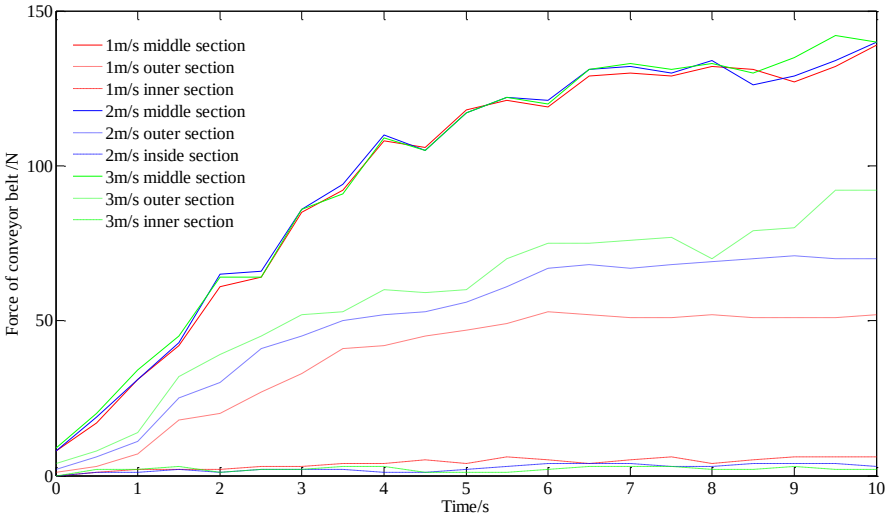

Fig. 7. Force curves of the outer, middle and inner side of the conveyor belt under different speeds

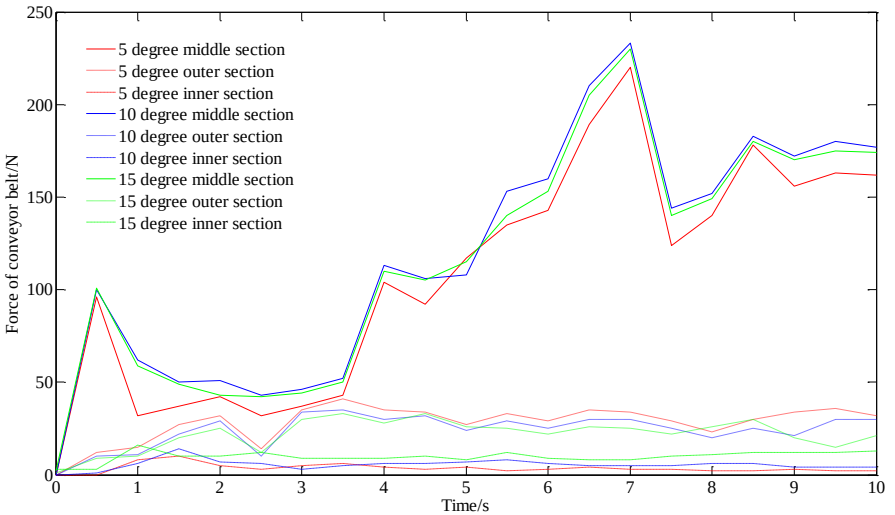

Fig. 8. Force curves of the outer, middle and inner side of the conveying belt under different internal curve elevation angle

4.3. Simulation results and analysis

When the inner curve elevation angle is 5 degrees, force curve of the outer, middle and inner side of the conveyor belt under different belt speed (1m/s, 2m/s, 3m/s) as shown in fig.7. When the belt speed is 3m/s, force curve of the outer, middle and inner side of the conveyor belt under different internal curve elevation angle as shown in fig.8. It can be concluded from the two figures, the force of the conveyor belt have a non-linear relationship with the speed of the belt and the elevation angle of the internal curve. The force of central region of the plane turning conveyor belt is the largest, the outside is the second, and the inner side is the smallest. This is consistent with the actual situation of the conveyor belt when horizontal turning. Along with the

increase of the belt speed and with the increase of internal curve elevation angle, the total force of the conveyor belt is gradually increased, which is consistent with the theoretical calculation results. It can be seen from the fig.7, when the belt speed is increased from 1m/s to 3m/s, the lateral force of the conveyor belt is gradually increasing, the middle of the conveyor belt is basically unchanged, the inner side of the conveyor belt is gradually reduced; And it can be seen from figure 8, when the internal curve elevation angle is increased from 5 degrees to 10 degrees, the lateral force of the conveyor belt is gradually decreased, the middle of the conveyor belt is basically unchanged, the inner side of the conveyor belt is gradually increasing.

Table 2 is simulation data of the total force of conveyor belt for coal transportation stable stage, when the belt speed is 3m/s and internal curve elevation angle is 15 degrees, the total force of the conveyor belt is 206N. While the belt speed is 1m/s and internal curve elevation angle is 5 degrees, the total force of the conveyor belt is 135N, which reduced 34.4%. This is consistent with the theoretical analysis.

Table. 2 Simulation data of the total force of the conveyor belt in the stable transport stage

Internal curve elevation angle	Belt speed (m/s)	Total force of the conveyor belt in the stable transport stage (N)
	1	135
5 º	2	147
	3	156
	1	152
10 º	2	177
	3	194
	1	182
15 º	2	191
	3	206

5. Conclusions

(1)In view of the size and the change of the load force of the conveyor belt at the turning point of the plane turning belt conveyor, the influencing factors of the stress of the conveyor belt at the turning point of the plane turning belt conveyor under full load condition are analyzed. The total force of the conveyor belt at the turning point is nonlinear with the speed of the belt, which increases with the increase of belt speed, and increment gradually increase. The total force of the conveyor belt is also nonlinear relation with the internal curve elevation angle, which decreases with the increase of belt speed, and the reduction is a trend of fluctuations.

(2) Using the discrete element simulation, the pressure curve of each supporting roller of the roller group at the turning point is analyzed. The force of the conveyor belt is in a non-linear relationship with the speed of the belt and the internal curve elevation angle. The force of middle area of the plane turning conveyor belt is the largest, the outside area is the second, and the inside area is the smallest. This is consistent with the actual situation of the conveyor belt when horizontal turning. The total force increases with the increase of the inner curve elevation angle, and increases with increase of the belt velocity, which is consistent with the theoretical calculation results.

(3) In the actual design of the plane turning belt conveyor, optimizing the belt speed and the elevation angle of the internal curve, which can reduce the pressure of the conveyor belt, improve the reliability and service life of the conveyor belt.

Acknowledgment

This research work was supported by the Emergency Management of National Natural Science Fund Project (Grant No.41542002), the First-Class General Financial Grant from the China Postdoctoral Science Foundation (Grant No.2013M540506) and Doctoral Fund of Ministry of Education of China(Grant No.20133415110003).

References

[1] ROCHA, A. V., FRANCA, G. J., DOS SANTOS, M. E., et al., 2012. Increasing long-belt-conveyor availability by using fault-resilient medium-voltage ac drives. *IEEE Transactions on Industry Applications*, 48(5), pp. 1708-1716.

[2] PANG, Y., LODEWIJKS, G., 2007. Simulation - based knowledge acquisition for intelligent belt conveyor monitoring. *Particle & Particle Systems Characterization*, 24(4), pp. 360-364.

[3] WANG, X., YANG, L., SONG, W., 2014. Structural analysis on freely turnaround idler combination at turning segment of belt conveyor with horizontal curves. *Mining & Processing Equipment*.22(3), pp. 268-273.

[4] TAO, MA ., 2013. Flat belt conveyor turning related technology research and dynamic simulation. *Taiyuan University of Science and Technology (Ph.D. Dissertation)*:43-51.

[5] LIBERWIRTH, H., 1994. Design of belt conveyors with horizontal curves. *Bulk Solids Handling*, 9(16), pp.66-71.

[6] GRIMMERK, J., KESSLER, F., 1992. The design of belt conveyors with horizontal curves. *Bulk Solids Handling*, 12(4), pp. 557-563.

[7] SUN, K., 1991. Transmission theory and design calculation of belt conveyor. Beijing: *Coal Industry Press*, pp. 214-238.

[8] SONG, W., 1996.Dynamic process research of large belt conveyor. *Journal of North-eastern university*,(1), pp. 65-68.

[9] SONG, W., ZHAN, Y., TONG, L., 2005. Calculation method of structural parameters of plane turning belt conveyor. *Chinese Journal of construction machinery*, 3(1), pp. 36-40.

[10] WANG, D., SONG W., 2005. Computer simulation of the starting process of the plane turning belt conveyor. *Journal of engineering design*, 12(1), pp. 28-34.

[11] PIAO, X., WANG, G., ZHANG, Y., 2007. Method for calculating the curvature radius of plane turning belt conveyor. *Coal mining machinery*, (3), pp. 5-7.

[12] LIU, B., 2013. The Design and Application of Long Distance Belt Conveyer with Horizontal Curves. *DaLian University of Technology (Ph.D. Dissertation)*:16-29.

[13] SONG, W., XU, Y., WANG, L., 2014. Simulation method of transport mechanism analysis of deep groove idlers belt conveyor in large inclination angle. *Journal of China Coal Society*, 39(S2), pp. 563-568.

[14] PIAO, X., 2010. Research on the key design technology of long distance flat belt conveyor. *Jilin University (Ph.D. Dissertation)*,33-39.

[15] KRUGGEL-EMDEN, H., SIMSEK, E., RICKELT, S., et al., 2007. Review and extension of normal force models for the discrete element method. *Powder Technology*, 171(3), pp. 157-173.

[16] LI, J., DU, C., XU, L., 2011. Impactive crushing and separation experiment of coal and gangue. *Journal of China Coal Society*, 36(4), pp. 687-690.

[17] ŽIVALJIĆ, N., NIKOLIĆ, Ž., SMOLJANOVIĆ, H., 2014. Computational aspects of the combined finite–discrete element method in modelling of plane reinforced concrete structures. *Engineering Fracture Mechanics*, 131, pp. 669-686.